Chapter 1
Structural Building Blocks of Soft Tissues: Tendons and Heart Valves

Himadri S. Gupta and Hazel R. C. Screen

Abstract Modelling the mechanical behaviour of soft tissues like tendon, ligament, skin and cartilage requires a knowledge of the structural and mechanical properties of the constitutive elements. These tissues have a hierarchical architecture from the molecular to the macroscopic scale, and are composites of different molecular building blocks. Here we first review the structure of the proteins and polysaccharides comprising such tissues. We then consider the structure and mechanical properties of two prototypical soft tissues: tendons and heart valves. An overview of their structure is followed by a description of the known mechanical behaviour of these tissues. Consideration is given to the role of different constituent components in mechanical response, structural anisotropy and testing methods which can probe mechanical deformation at multiple levels.

1.1 Structural Components of Soft Tissues

Connective soft tissues like tendon, cartilage, skin, ligament and arteries are required to resist a range of mechanical loads as part of their normal physiological function. These mechanical requirements exhibit considerable variation: for instance, tendon is built to resist uniaxial loading, skin to provide a structural barrier against the environment and against multidirectional loads, while cartilage provides frictionless sliding and compressive resistance at the ends of bones [1]. These properties are critically enabled by the structure and architecture of the extracellular matrix (ECM) which is secreted by cells such as tenocytes and chondrocytes.

By themselves, the mechanical properties of cells (∼kPa) are far too low to enable effective resistance to the typical loads of a few MPa that are experienced *in vivo*. Cells must therefore secrete a range of biological macromolecules—both proteins and polysaccharides—which self-assemble into fibrils, lamellae and fibre bundles to form

H.S. Gupta (✉) · H.R.C. Screen
School of Engineering and Materials Science, Queen Mary University of London,
Mile End Road, London E1 4NS, UK
e-mail: h.gupta@qmul.ac.uk

S. Avril and S. Evans (eds.), *Material Parameter Identification and Inverse Problems in Soft Tissue Biomechanics*, CISM International Centre for Mechanical Sciences 573, DOI 10.1007/978-3-319-45071-1_1

the ECM. The structural diversity of the motifs formed [2] are the key which enable such tissues—made out of mechanically relatively unimpressive components—to achieve impressive adaptation and optimization to their *in vivo* loading regimes [3].

In this chapter, we first review the structure and properties of common molecular building blocks of soft tissues. We then identify some common structural and mechanical motifs that appear repeatedly, with different constituents, across biological materials. Finally, we describe the specific properties of two prototypical soft tissues: tendons and heart valves, and relate how structure enables mechanical behaviour, to the extent currently known.

1.1.1 Hierarchical Structure of Proteins

The most common proteins in soft tissues, by decreasing frequency of occurence, are collagen, elastin and fibrillin. The proportions of these components can vary considerably between the tissues of origin: skin, tendon, arteries, lungs and heart valves. The primary structure of collagen-like and elastin-like proteins are distinct. While collagens are characterized by a predominance of the repeating amino acid triplet glycine-X-Y (where X and Y are either proline or hydroxyproline) elastin contains 30 % glycine with the majority of other amino acids being valine, alanine or proline [4, 5]. The secondary structure of collagens is a triple helix, while elastin-like proteins consist of alpha-helices and beta-turns. In both, the covalent cross-linking is through lysine residues.

Collagen: Collagens consist of triplets of polypeptide chains (known as α-chains), with each chain characterized, at the level of primary structure, by a repeating of the triplet (Gly-X-Y), where Gly stands for glycine and X- and Y- are most commonly either proline or hydroxyproline. This characteristic repeat, together with the small size of the glycine residue, results the chains forming a tight right-handed triple helical conformation, with the glycine residue on the interior of the helix [6]. Over 29 different types of collagens are known, which can be divided (from a bioengineering viewpoint) into fibril-forming and non-fibrillar collagens. The fibrillar collagens—mainly Type I–III as well as smaller proportions of type V and IX—are structurally the most significant contributors to the mechanics of soft tissues acting as stiff fibrous units within tissues. Collagens may be classified as homotrimeric (where the three α-chains are identical, as in Type II and III) or heterotrimeric (where not all the α-chains are identical, as in Type I). These are denoted via the shorthand notation $[\alpha 1(I)]_2\alpha 2(I)$ (for Type I) and $[\alpha 1(II)]_3$ (for Type II). These fibrillar collagens comprise a triple helical central region, typically around 1000 residues long (or 330–340 (Gly-X-Y) triplets), with non-helical ends at the C- and N-termini. Collagen I is the most commonly found variant in tendon and heart valves, the focus of this chapter.

At the nanometre length scale the individual tropocollagen molecules assemble into insoluble fibrils, which are (for Type I collagen) typically in the 50–200 nm diameter range. Fibril-associated collagens (FACITs) are found typically on the surface of the fibrils. Collagen molecules typically aggregate in a highly regular manner both axially (along the length of the tropocollagen helix) as well as laterally (side-by-side packing of the helices). This results in a characteristic banding pattern with a D = 65–67 nm pattern visible in electron or scanning probe microscopy as well as in small-angle X-ray diffraction, which arises from the repeated staggered arrangement of molecules. Adjacent tropocollagen molecules are laterally shifted by D, to maximize contact between hydrophobic regions. Since the length of a tropocollagen molecule is 300 nm, which is not an integral multiple of D, the lateral stagger leads to regions of high and low electron density inside the array of tropocollagen molecules comprising the fibril. The D-period is sensitive to hydration, with dry collagen having a D-period of 65 nm and wet collagen 67 nm. There are about 234 amino acids per D-period repeat [7]. In vertebrates, collagen fibrils are synthesized with relatively short lengths (1–3 μm) initially, and form much longer fibrils of unknown length by the process of axial fusion. In certain tissues like skin, branched networks of fibrils are also formed [8].

The fibril is often classed as the fundamental building block of tissues, and in different tissue types, it further aggregates into fibres or bundles. At the scale above individual fibrils, aggregation into fibre bundles, lamellae or fibres occurs depending largely on the tissue type. In tendons, characteristic fibres of diameter of the order of tens of microns are present [9], while in mineralized collagenous tissues lamellae of fibrils in a plywood arrangement are characteristic [10]. Considerable inter-tissue variation is present.

Elastin: Elastin is a stable, insoluble and rubbery protein [2, 4] which comprises the bulk (>90 %) of elastic fibres in tissues like skin, ligament, arteries and lung. The insolubility of elastin arises from extensive lysine cross-linking between adjacent elastin molecules. The mechanics of elastin networks is driven primarily by entropic elasticity [11], as they are far more rubber-like in conformation compared to collagen fibrils. Analogues of elastin are found in a range of phyla: lamprey cartilage and mussels have proteins which have similarities to elastin [4]. Tropoelastin is the soluble precursor of elastin and contains two types of domains: hydrophobic domains with nonpolar amino acids (glycine, valine, proline and alanine) [4] and hydrophilic domains contain lysine and alanine. Hydrophilic domains are involved in cross-linking of adjacent elastin molecules. Similar to the process of fibril formation, microfibrils of elastin are formed in the extracellular compartments adjacent to the secreting cells and are rapidly cross-linked. Fibre diameters show some variability: intervertebral disc and cartilage have thin fibres <1 μm, while in the ligamentum nuchae fibres of ∼1 μm are comprised of subfibrils of 200 nm diameter [11]. These fibres are arranged into larger scale lamellae, as seen in aortic media. Figure 1.1 from [12] shows the differences in structure between the elastic fibrils in arteries and in ligament.

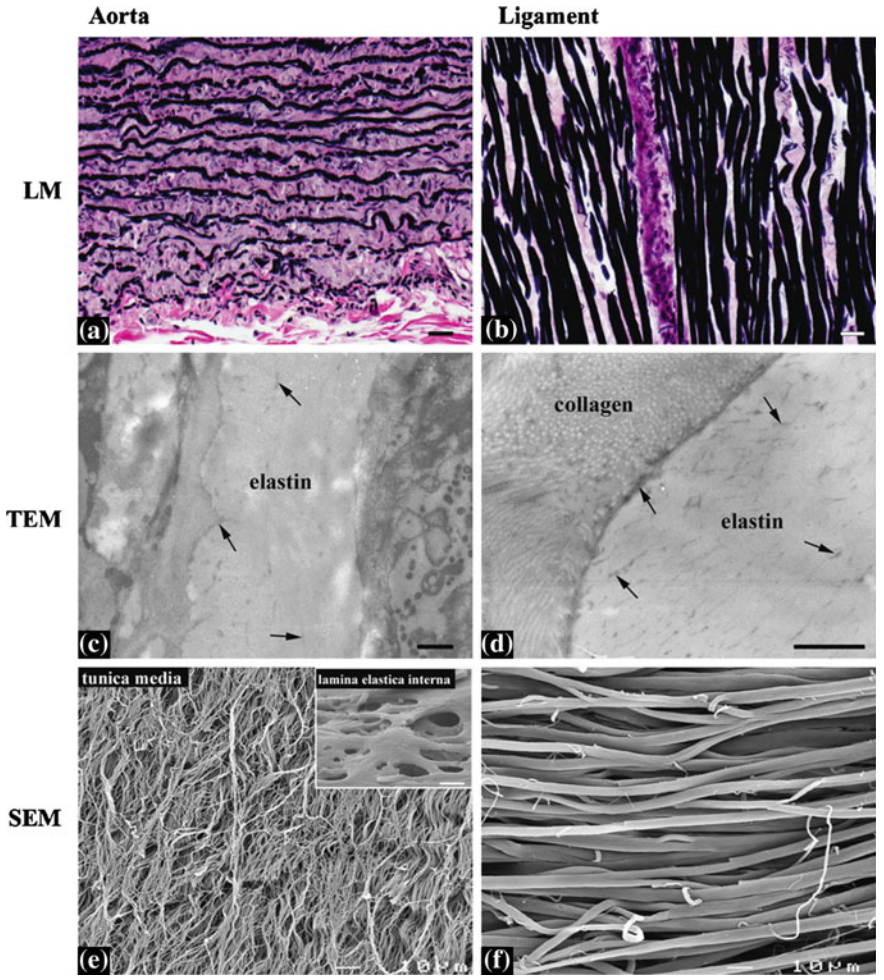

Fig. 1.1 Images of elastin fibres in aorta **a** and ligament **b**, taken with permission from [12]. The *top row* **a**–**b** shows light microscopic images of stained (Verhoeff-Van Gieson) tissue; elastic fibres are black while collagenous tissue is pink. *Middle row* **c**–**d** report transmission electron microscopy images from the same tissues and the *lowest row* **e**–**f** shows scanning electron microscopy (SEM) images. A thinner fibre diameter, and less ordered fibrous arrangement, is evident in the aorta

1.1.2 Hierarchical Structure of Polysaccharides

Polysaccharides consist of aldoses and ketoses, and are characterized by the general formulae $C_n(H_2O)_n$. They include mono-, oligo- and polysaccharides. Monosaccharides are the basic building blocks, an example of which is glucose ($C_6(H_2O)_6$). They can form disaccharides (with two monosaccharides) or oligosaccharides (between three and ten), which are monosaccharides combined via a glycosidic linkage.

Monosaccharide chains with more than ten monosaccharide units are denoted as polysaccharides, and include widespread materials like starch, chitin or cellulose.

Polysaccharides can form fibres (as in chitin) but in soft tissues are more commonly found in gel-like phases coexisting with the stiffer protein-based fibrous networks of collagen and elastin. These will now be briefly described.

Chitin: Like proteins, polysaccharides can also display a hierarchical structure: the chitin within the cuticle in arthropod skeletons, for instance, is comprised of α-chitin fibrils in a protein matrix, aggregated into fibres and lamellae [2, 13]. Indeed, at least five levels of hierarchy have been identified in chitinous tissues [14] which serves as an example of a structural biomaterial with polysaccharide (chitin) fibres as a principal building block. At the macroscopic scale, there are three layers to the cuticle: a thin outer epicuticle, a calcified exocuticle, and a less dense endocuticle, which have thicknesses of the order of a few hundred microns. The exo- and endocuticle are comprised of lamellae of chitin fibres, which undergo a 180° rotation around the axis perpendicular to the cuticle surface within each lamella. At this scale, a second phase of fibres running perpendicular to the lamellae have been identified. These fibres are found in pore canals which form a honeycomb-like structure together with the lamellae [2, 13]. The fibres have diameters between 50 and 250 nm, and are in turn comprised of 2–5 nm diameter chitin fibrils together with a mixture of crystalline and amorphous calcium carbonate and an amorphous protein phase. The fibrils comprise of several chitin molecules aggregated in an antiparallel manner and wrapped by protein. The multiple hierarchical levels are shown in Fig. 1.2.

Glycosaminoglycans and proteoglycans: Glycosaminoglycans (GAGs) like hyaluronic acid are large, unbranched polysaccharides which form a gel-like phase coexisting with the fibrous proteins in soft tissues like tendon, cartilage and ligament. They are typically highly hydrophilic with a negative charge density, and as a result attract cations like Ca^{+2} or Na^{+}. Hyaluronic acid (often abbreviated HA) is a polysaccharide with molecular weight between 10^5 and 10^7 Daltons, containing about 10^4 disaccharides. The building blocks of HA are *N*-acetyl-D-glucosamine and D-glucoronic acid.

GAGs are most typically found in the form of proteoglycans, which consist of a core protein chain with GAG chains branching off from the core. Proteoglycans play an especially important mechanical role in resisting compression and shear in tissues such as cartilage and the annulus fibrosus of the intervertebral disc, due to their negative fixed charge density and consequent swelling pressure. In addition, their hydrophilic nature increases the water content of the tissue, thus also increasing osmotic pressure. Examples of PGs are aggrecan and decorin. Aggrecan is typically about 400 nm in length, with chondroitin sulphate GAG chains branching off from the core protein with a length of 40 nm and globular domains at the end (*CITE*). It has a molecular weight of ∼225–250 kDa. Decorin is a much smaller PG, and a member of the SLRP family. It has one GAG chain (either dermatan sulphate or chondroitin sulphate).

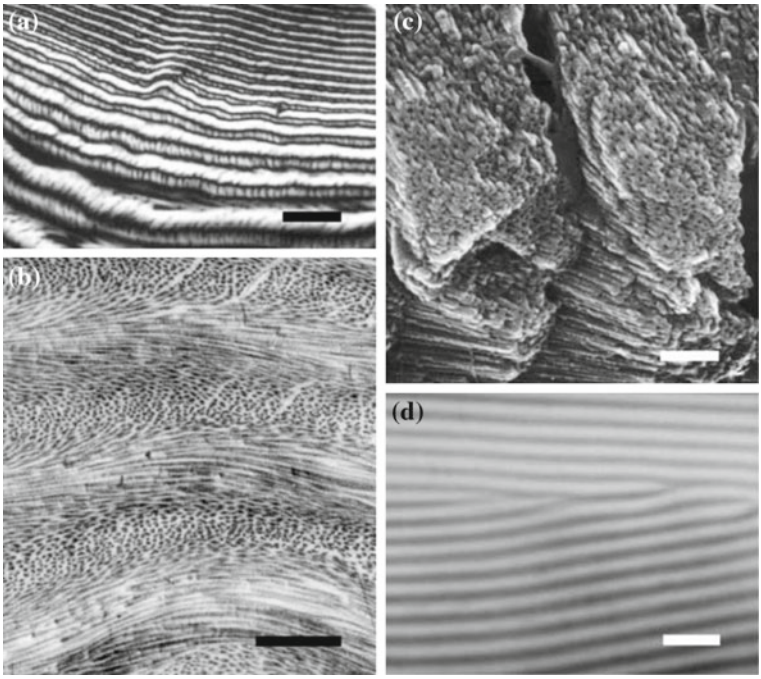

Fig. 1.2 Chitin fibre networks from crab cuticle and synthetic chitinous materials, image taken with permission from [15]. Image **a** reports polarized light microscopic imaging (scale bar is 20 μm). **b** The cholesteric liquid crystal arrangement within a single lamellae, seen from electron microscopic imaging of sections of cuticle, where fibres at different angles to the sectioning plane appear as oblique or perpendicular to the plane (scale bar is 1 μm). **c** Shows an image of (undecalcified) cuticle, where a calcium carbonate phase is present along with the fibrils (scale bar is 0.2 μm). **d** An example of synthetic colloidal suspensions of colloidal chitin, imaged with polarized light microscopy, with the banding characteristic of the lamellar structure shown (scale bar is 100 μm)

1.1.3 Design Principles of Biological Materials

Structural organization of the fibre–matrix in different patterns The relatively restricted set of biopolymers described in Sects. 1.1.1 and 1.1.2 of this chapter are used by cells in soft tissues to build ECM with a wide range of mechanical properties and structural motifs [2]: from the compressive and sliding resistance of cartilage, to the fatigue resistance of tendon and heart valves or (considering biomineralized tissues) the toughness of bone and related calcified tissues. Biologists may concern themselves with questions relating to rates of cell secretion of ECM matrix, rates of removal and turnover and whether these can be manipulated in synthetic or *in vitro* conditions to build tissues in a biomimetic manner (the domain of tissue engineering). However, the bioengineer may have equal if not greater interest in understanding how these building blocks self-assemble to optimize certain mechanical properties.

Broadly speaking, the types of ECM molecules described above are usually found in fibre composite arrangements, implying fibrouse and gel/matrix phases, usually in close spatial association (at multiple levels). Fibres are used to provide high stiffness and strength, whilst matrix phases can both transfer forces between fibrils as well as provide stability to the fibres and bind or stabilize the water phase. We will now consider, from a structural perspective, fibre composite designs as found in several soft tissues, and discuss which particular mechanical property will be optimized for a given arrangement.

In Fig. 1.3a, the same fibre–matrix arrangement is shown in three different orientations with respect to the loading direction. In the first, the fibres are parallel to the loading direction, and as a result the material is expected to be stiff and exhibit high elastic recovery. Conversely, if the load is applied perpendicular to the fibre long axis, the soft and viscous matrix phase (which corresponds to the PG/GAG rich interfibrillar material) will dominate the strain response, leading to less elastic recovery and a more compliant material. Finally, when the fibres are at an angle to the loading direction, the fibres will bear (approximately) the projection of the force

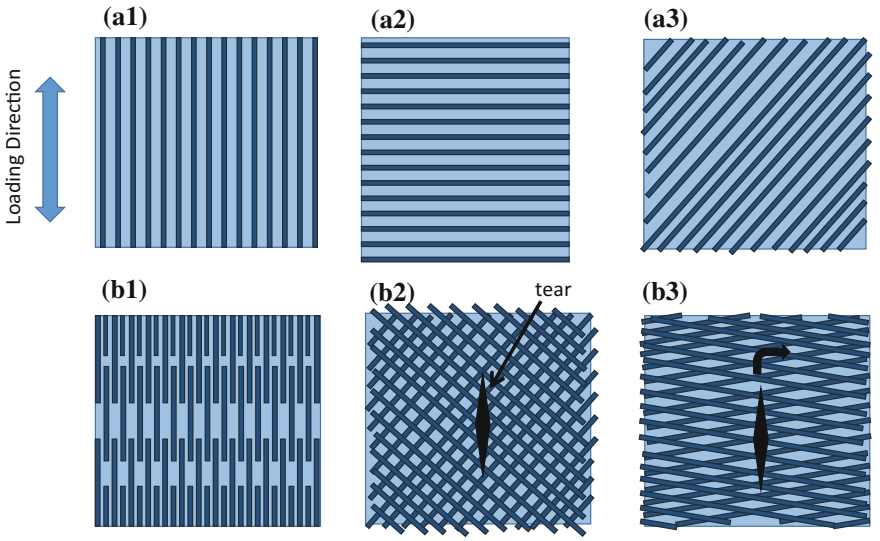

Fig. 1.3 **a** Fibres (*dark blue*) inside a ductile matrix (*light blue*) mimicking the fibre composite structure found in numerous soft tissues. If the loading direction is as indicated by the *arrow*, the fibres will bear the tensile load in the left image (Voigt loading as in [16]), while very little load in the centre image (Reuss loading as in [16]). In the middle image, depending on the degree of viscosity and stiffness of the matrix, fibres will reorient toward the loading direction. **b** *Left* Finite length of the fibres implies interfibrillar shear transfer through the matrix. *Middle* By having multiple fibre orientations (as in skin or arteries), crack propagation can be hindered, as there will always be a proportion of fibres which need to be fractured (with high breaking stress) for the crack to propagate. *Right* A schematic of the fibre geometry as found in arteries, where resistance to circumferential loading is most important. Cracks will be diverted from the initial direction to run in the "weak" direction between fibres rather than across them

onto the fibre axis, but may also be induced to rotate in the matrix toward the loading direction. When the length of fibres is reduced (Fig. 1.3b1) the contribution of the matrix to material mechanics is increased, as in this case the force is not borne end to end (in the tissue) by the fibre, but is transferred (via shearing mechanisms [16]) through the viscous matrix. By controlling the degree of overlap of the fibres, as well as the interfibrillar matrix spacing, the effectiveness of the shear transfer can be controlled.

Whilst aligned fibres are beneficial in some tissues such as tendon, in many tissues, loading is multidirectional, lending itself to fibre arrangements, such as Fig. 1.3b2. Matted or plywood-like structures will achieve stiffness in multiple directions (as there are always a proportion of fibres along the loading direction), and can limit the extent of fibre reorientation. However, such an arrangement provides the additional benefit that cracks cannot propagate easily through the material (incidentally, this is true in both loading directions), because such a propagation will require reaching the high tensile strength of an individual fibre, thus making the material tough.

These idealized structures are surprisingly close to the fibre–matrix architectures found in soft tissues. Figure 1.3b1, for example, is a close match (at both the fibre and fibril level [9]) for the structure of tendon. Similarly, Fig. 1.3b2 can be found in both skin and arteries. In skin, the planar structure of the tissue and the requirements for resistance to multidirectional loading mean that an isotropic fibre distribution maximizes both strength and toughness. Fibre arrangement is a tradeoff—the toughness brought about by multidirectional fibres against the need for tensile strength in a certain loading direction—and hence in arteries, where high strength is required (Fig. 1.3b3) an orientation of fibres in the circumferential direction provides increased strength, but at the risk of damage propagation in that direction.

Fibre composite theory The shear transfer between fibres and matrix is a problem that materials engineers have considered since at least the 1950s, initially in relation to the paper-making industry through the work of Cox [16, 17]. The simplest model which is presented in textbooks is the "shear-lag" model [16, 17]. This model attempts to describe how effective a fibre is in increasing the stiffness of a (compliant) matrix in which it is placed. It gives quantitative estimates of the minimum length needed for the stress on the fibre to reach its maximum value (limited by the tensile strength of the fibre); fibres which are shorter than this are clearly not as effective as they could be in maximizing the stiffness of the ECM composite they are part of. This concept is captured by the idea of the critical fibre length, which is the minimum length necessary for all the force applied through the matrix to be transferred to the fibre, and is given by $l_c = \sigma r/\tau$ where r is the radius of the fibre, σ is the maximum tensile stress, and τ is the shear in the matrix.

In the shear-lag model, the ends of each fibre are free of normal stress, which builds up progressively toward the centre of the fibre (Fig. 1.4b, c). As a result, the contribution of the fibres to the maximum force is reduced. While in the case of infinitely long fibres with a volume fraction V_f, the elastic modulus is given by the serial or Voigt expression

$$E_c = E_f V_f + E_m(1 - V_f) \tag{1.1}$$

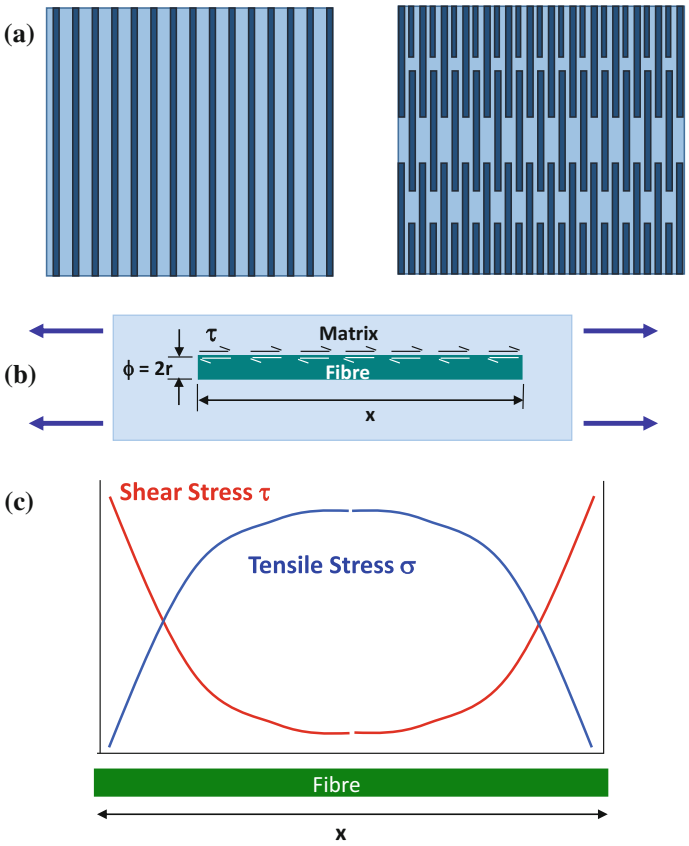

Fig. 1.4 Shear-lag model of fibre load transfer: *Top row* shows that when the fibre length no longer extends across the entire specimen, some degree of interfibrillar load transfer through the interfibrillar matrix is necessary. *Middle* Schematic of a single fibre (*dark blue*) in a matrix (*light blue*), showing the shear τ acting across the length x of the fibre. In response to a far-field load (*arrows* on the left and right of the schematic), a progressive build up of axial fibre stress (*blue line*) occurs, with the ends of the fibre being free from axial stress. The shear stress (*red line*) is maximum at the ends and (by symmetry) is zero at the centre of the fibre. If the fibre is long enough, the maximum axial strength of the fibre can be reached in the middle region of the fibre

where f is for fibre, m is for matrix, and c is for composite.

In a composite with fibres of finite length a correction factor $V_f(z) < V_f$ is necessary [1]. Specifically, the modulus of the composite is

$$E_c = E_f V_f(z) + E_m(1 - V_f) \tag{1.2}$$

where z is a correction factor dependent on the shear modulus of the matrix G, the elastic modulus E and the radius and length of the fibre. The correction factor accounts for the imperfect bonding and progressive shear transfer across the length of the fibre.

Hierarchical organization and toughness As the soft tissues discussed here can be considered fibre composites at different hierarchical levels, it is worth considering how the fibre–matrix interaction changes across the hierarchy and the effect this may have on toughness. In general, for soft tissues, it appears that at the lowest length scale (fibrils in tendon, for example) the bonds between fibril and matrix is quite strong, leading to homogeneous strain fields in low stress deformation. However, at higher stress levels, when cracks or damage may appear in the material, weak interfaces at higher length scales (such as between the fibres or fascicles in tendon) play an important role in making the tissue notch-insensitive and as a result tough.

Another strategy to increase toughness [1] is the use of holes at different length scales. Such an approach is more common in tissues such as wood and plant cells or in bone, and will only be briefly discussed here. The idea is that holes can act to blunt or deflect oncoming cracks, and create extensive tortuous crack paths. The reduction of stress-concentrations caused by crack blunting will prevent further cracks from occurring and is known as the Cook-Gordon crack stopping mechanism [1]. Naturally, too many holes would weaken the material, so a balance has to be maintained. It is worth noting that such "holes" (like the pore canals in cuticle or the vessels in plant xylem) usually have a transport function (of water and nutrients) of their own.

Prestress and pre-strain: While the protein (and polysaccharide)-based fibres described above are excellent in resisting tension, the presence of water in most soft tissues is utilized to increase resistance to compression. First, the GAG/PG-rich gel described in previous sections is hydrophilic and has a high negative fixed charge density, as a result of which the water is stabilized within a gel-like phase interpenetrated by a web of fibres in tension. The tissues may be considered as fibre-linked containers, where the collagen (and other) fibrils restrain the swelling pressure of the gel. As a result, the fibrils are in constant tension or a state of pre-strain. The role of prestress and pre-strain has been well-established for arteries [18], and is a critical component of fibril reinforced models for cartilage [19]. Alterations in swelling pressure in the ECM due to reduction in fixed charge density are also implicated in the reduction of the load bearing capacity of the nucleus pulposus of the intervertebral disc [1].

1.2 Structure and Function of Tendons

1.2.1 Function of Tendons

Tendons are designed to transmit forces between muscles and bone [20]. Long tendons remove the need to have muscles placed close to the joints. As a result of these requirements, they need to be relatively inextensible (failure strains of around 10–20 %), as well as absorb impact forces encountered during gait. Some tendons are additionally elastic to enable storage of energy during locomotory gait. Ligaments, in contrast to tendon, connect two bones, rather than bone to muscle, preventing large torsion or twisting between joints.

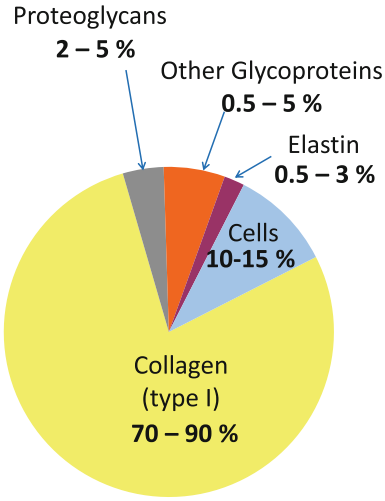

Fig. 1.5 Pie chart showing composition of tendon with approximate percentages of different molecular constituents

The main components of tendon and ligament are shown in Fig. 1.5. Collagen (at 70–90 %) is by far the most plentiful constituent, while the next most abundant components (proteoglycans and other glycoproteins) account for less than 10 % of the tissue. A small proportion of elastin is also present. The range of glycoproteins present can be quite diverse, including decorin, aggrecan, versican, fibromodulin, lumican, tenascin-C [21], COMP (Cartilage Oligomeric Matrix Protein) and lubricin [22, 23]. However, decorin usually dominates in most tendons. Cells account for the remaining 10–15 %, highlighting that tendon like many connective tissues is a largely acellular tissue [20, 24, 25].

The structure of tendon is in many ways a prototype of the hierarchical structures of other more complex soft tissues like arteries and heart valves. A schematic of the structure is shown in Fig. 1.6, adapted from [26]. It is observed that tendon can be considered an aligned fibre composite at multiple levels, and that a characteristic motif of "stiff-fibres/ductile matrix" is observed at multiple levels from the

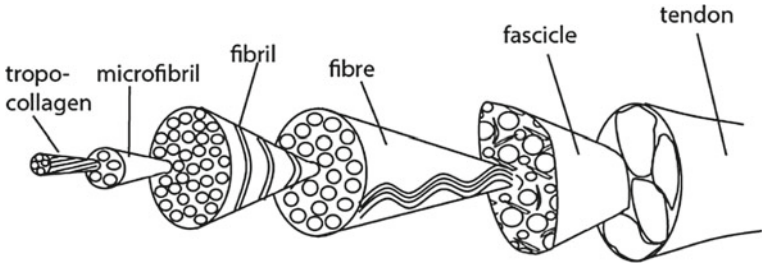

Fig. 1.6 Hierarchical architecture of tendon, adapted from [34]. Collagen aggregates, from the molecular level of the tropocollagen molecule, up through the nanometre scale fibril, microscale fibres to the mesoscale fascicle and entire tendon tissue

nanoscale to macroscale. Interspersed inside the ECM composite are the tenocytes (or ligamentocytes) [26, 27].

At the smallest scale, we have the tropocollagen molecules with diameter 1.5 and 300 nm length [28]. These are tightly cross-linked into microfibrils [29]; diameter (~3–4 nm) and fibrils (diameters between 20 and 200 nm depending on species, maturity and tissue location), with increased collagen fibril area also a predictor for age in tendons [30]. In between the fibrils is a proteoglycan-rich matrix, with decorin among the PGs which bind to adjacent fibrils [31]. This fibril/matrix motif repeats itself at the next higher level of fibres (10–50 μm diameter) and fascicles (50–400 μm) where tendon cells (tenocytes) are interspersed in rows between fibres and fascicles along the tendon [9]. At the tissue level, fascicles (visible to the eye) are surrounded by interfascicular matrix or endotendon, and bound together to make tendon [26].

Certain features of the fibre–matrix arrangement occur at multiple length scales: for instance, crimped structures are visible both at the fibrillar level and the fibre level. It is noted that tendon is poorly vascularized, and the blood vessels that are present are between fascicles. The matrix between fascicles, which is termed the interfascicular matrix (IFM), contains loose connective tissue matrix, with a higher amount of collagen type III, elastin and proteoglycans such as lubricin [32]. Whilst a generic tissue structure and composition has been presented, ligaments and tendons differ somewhat in composition. In general ligaments have somewhat lower collagen content, greater fraction of elastin and have a more weave-like structure [33]. However, it is notable that tendons vary widely in composition in order to adapt their mechanical behaviour to meet their functional need, emphasizing the exquisite capacity for our tissues to utilize their complex hierarchical arrangements to adapt to mechanical needs. Certain features of the fibre–matrix arrangement occur at multiple length scales: for instance, crimped structures are visible both at the fibrillar level and the fibre level. It is noted that tendon is poorly vascularized, and the blood vessels that are present are between fascicles. The IFM contains loose connective tissue matrix, with a higher amount of collagen type III, elastin and proteoglycans such as lubricin [32]. Whilst a generic tissue structure and composition has been presented, ligaments and tendons differ somewhat in composition. In general, ligaments have somewhat lower collagen content, greater fraction of elastin and have a more weave-like structure [33]. However, it is notable that tendons vary widely in composition in order to adapt their mechanical behaviour to meet their functional need, emphasizing the exquisite capacity for our tissues to utilize their complex hierarchical arrangements to adapt to mechanical needs.

1.2.2 Specialized Regions of Tendon–Ligament

The osseotendinous junction is a mechanically crucial interface between tendon and bone [35]. Owing to the very different mechanical properties of bone (~20 GPa Young's modulus) and tendon (~1–2 GPa), a functionally graded transition is needed

between the two organs. It is clinically relevant as it is a potential weak point in structure, and prone to injury. It is characterized by a linear increase in mineral concentration across the junction, a transition zone with type II collagen and a loss of the predominant collagen orientation in tendon. Analogous structures include the interface between muscle and tendon (where mechanical differences are less pronounced), known as the myotendinous junction, characterized by an interdigitation of muscle and collagen fibres.

1.2.3 Mechanical Properties of Tendon and Ligament

The mechanical properties of tendons and ligaments in tension (the most relevant loading mode) can be considered in comparison with standard man-made materials like metals or rubbers. Typical stress–strain curves for metals and rubbers are shown

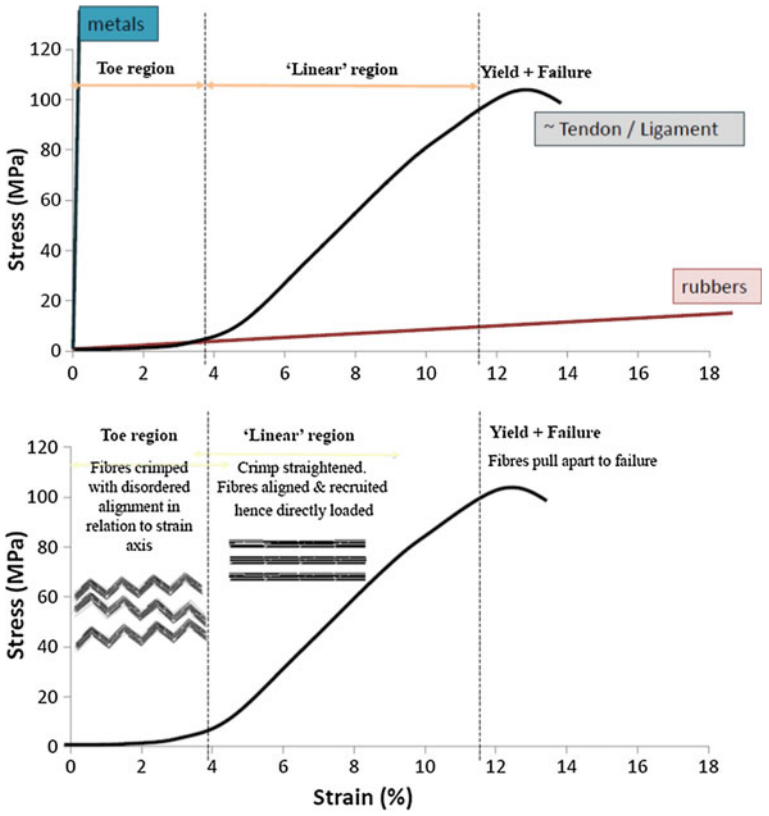

Fig. 1.7 Comparison of the stress–strain curve of tendon, in tension, with that of metal (*left*) and rubbers (*right*). In the lower graph, the three different strain regimes: toe, linear and yield are indicated together with a brief description of the structural changes

in Fig. 1.7a, with—in comparison—a typical stress–strain curve for tendon. It is observed that the maximal deformation of tendons (~10–20 %) is much larger than the yield strain of metals (~1 %) and much smaller than the ~500 % failure strain in rubbers. Characteristic features of the stress–strain curve in tendon are an initial *toe* and *heel* region up to ~4 %, a nearly linear increase of stress with strain from ~4–12 % and a short yield and failure region thereafter. The tangent modulus in the linear region is ~1–2 GPa, much lower than ~100 GPa range for metals, but larger than the <1 GPa moduli in rubbers.

Considerable attention has been paid to understanding how the hierarchical structure described in the previous sections can lead to the aforementioned mechanical behaviour, and a fairly complete understanding of at least the main mechanisms are now known (reviewed in [36]). In the toe region, the tendon starts out in a macroscopically crimped configuration (these crimps are visible under the light microscope). The removal of these crimps plus alignment of collagen in loading axis occurs over the toe region with nearly no increase in tissue stress. However, the initial nonlinear increase of the stress just after the toe region (the heel region) involves smaller structural units in the hierarchy. Misof et al. [37] proposed the involvement of molecular level vibrations, lateral to the force direction, by analyzing the changes in the X-ray diffraction intensity arising from the lateral packing of the collagen molecules. In their model, an lateral vibration in the gap regions of the tropocollagen molecules is reduced in amplitude on deformation, explaining the alterations in X-ray scattering intensity; this "rubber-like" contribution to the internal free energy thus influences the stress–strain curve in the heel region.

In the linear region, the crimps (and smaller scale structural features) are straightened and fully aligned with the loading direction so the fibres now are fully recruited to bear the load [38]. In this region at the ultrastructural level, the consensus is that some degree of inter- as well as intrafibrillar sliding, coupled with elongation of the tropocollagen molecules, occurs [39, 40]. These mechanisms can be quantified by analyzing peak shifts in X-ray diffraction patterns arising from meridional packing of collagen molecules in the fibrils. The deformation remains regular, i.e. a similar intra- and interfibrillar structural rearrangement occurs across the tissue over the fibrils. Recent data demonstrates that sliding also occurs between fibres and fascicles, and the relative contributions of sliding through the different hierarchical levels of the tissue can be modulated by altering the matrix composition and subsequently its mechanical properties at different levels in the hierarchy. Finally, fibres pull apart and fracture in the nonlinear and fracture region [34].

Given that tendon (and ligaments) are subjected to time-dependent loading over most of their lifetime, it is of equal importance to understand the viscoelastic mechanical behaviour. The simplest types of tests for understanding viscoelasticity are stress relaxation (holding the tissue at a constant strain and monitoring the reduction in stress) and creep (holding the tissue at constant load and measuring elongation). Creep in tendon can be categorized into the initial rapid (primary) creep, followed by a slower (secondary) creep and eventually by a very rapid tertiary creep which leads to failure [41]. It is observed that creep behaviour changes with age; in particular, the duration of secondary creep and extent of sample elongation is much longer

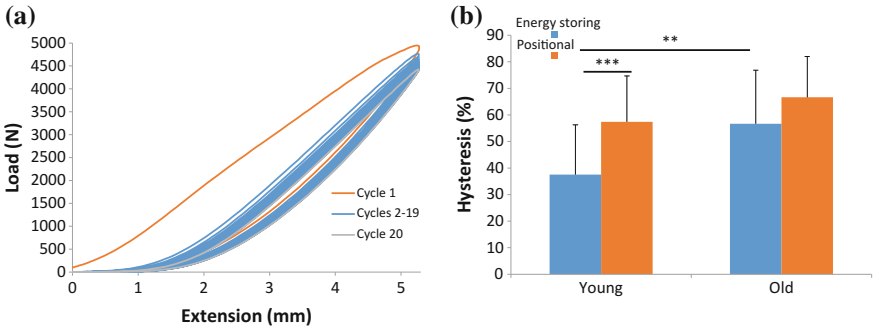

Fig. 1.8 **a** Cyclic loading of tendon leads to viscoelastic energy loss, measured by the hysteresis (% of area between loading and unloading cycles). **b** The degree of hysteresis is lower in energy storing versus positional tendons

in older tendons, likely due to an increase in intra- and interfibrillar cross-linking. Another important parameter for viscoelastic behaviour is the energy loss during cyclic loading (Fig. 1.8, left). The degree of hysteresis (area between the loading and unloading curves) is a parameter characterizing the extent of energy loss. The degree of hysteresis in cyclic tensile loading of tendon is dependent both on the age of the tendon as well as the type of tendon. For example, energy storing tendons show a smaller hysteresis than positional tendons (Fig. 1.8, right).

1.2.4 Hierarchical Analysis Techniques

The hierarchical structural elements (from fibrils at the nanoscale to fascicles at the macroscale) affect the mechanics of tendon and related tissues in distinct ways. Different experimental techniques—both mechanical as well as imaging-based, and some combining the two—need therefore to be applied or developed to understand the micro- and nanoscale mechanics. At the molecular and the nanoscale, methods to probe mechanical deformation include X-ray diffraction (to measure helical pitch in tropocollagen molecules) [43], Raman spectroscopy (to identify different functional groups like amides in the protein and to observe stress-induced shifts) [44], small-angle X-ray diffraction to measure the fibril D-period [39, 40, 42, 45, 46]. These are generally employed to visualize sample strain response, whilst the tendon is strained within an appropriately designed loading rig. Techniques like atomic force microscopy and microelectromechanical-sensors (MEMS) have also been utilized to deform individual collagen molecules and fibrils [47]. In addition, the use of *ab-initio* molecular dynamics simulations for studying deformation of individual collagen molecules as well as small aggregates of molecules (proto-fibrils) should also be mentioned [48], with the proviso that the short timescales (of the order of nanoseconds) in molecular dynamics necessarily make the mechanical testing

timescales in such computational studies quite far from those used in most laboratory tests as well as in *in vivo* testing.

These sub-micron scale mechanical test methods are complemented by high-resolution imaging methods like electron microscopy in order to help correlate local mechanics with tissue structure. Between the microscale and the macroscopic scale, however, there are a lesser number of well-established methods for mechanical testing linking structure to mechanics. Examples of techniques which have been applied at this scale are confocal microscopy, digital light microscopy and photography, usually in combination with mechanical testing methods. These are complemented by standard biological imaging methods like histology and histochemistry combined with light microscopy. At the macroscale, real-time mechanical testing methods include image correlation techniques, photography and polarized light microscopy: it is observed that there is some overlap of methods with the sub-mm scale mentioned above, but the analysis is usually at a lower level of resolution and presents fewer problems with interpretation.

We consider first the deformation at the macro- and microscale. Examples of use of photography to image different stages of the tensile deformation of tendon are shown in Fig. 1.9 from [9]. The change in the crimp structure (left) can be seen, as well as the straightening of fibres in the linear region. The fractured, rough surface of the tendon at rupture likewise indicates a sliding of fibres as they shear past one another as the

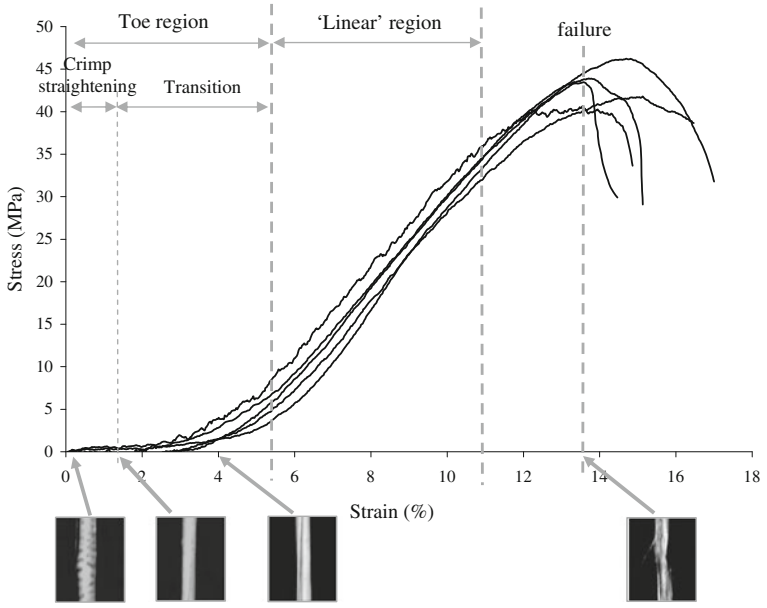

Fig. 1.9 Five prototypical stress–strain curves of rat-tail tendon, strained to failure at 1 mm/min. *Lower* frames show video capture photos at progressively increasing strain levels. Data and figure from [9]

tendon fails. At one scale below this, confocal microscopy combined with *in situ* testing of tendon samples can image the deformation of fibres and fascicles [9, 49] within tendon as the samples are strained. By tracking cell displacement within the tissue, or directly staining and visualizing collagen within samples, the fibre extension and interfibre sliding can both be measured. It has been found that the fibre extension is considerably less than interfibre sliding, indicating considerable shear between the fibres [9]. Interestingly, some degree of hysteresis is observable at both the inter- and intrafibre level [50]. We note that recently, a variant of notch-tensile testing used on tendons to obtain the interfibrillar shear stresses has been developed. This is a novel application of a macroscale test methodology to obtain fibrillar level mechanical parameters [51], and confirms shear transfer between collagen units through the tendon hierarchy.

At the fibrillar level, using small-angle X-ray diffraction (SAXD), the D-periodic variation of the electron density along the axis of the fibril generates a set of Bragg peaks along the orientation of the fibril. Use of high brilliance synchrotron radiation enables rapid acquisition of SAXD frames, within a few seconds [39, 40, 42, 45, 46]. When a microtensile tester containing tissue in a fluid chamber is mounted in a synchrotron SAXD beamline, concurrent application of mechanical test protocols like uniaxial stretch to failure, stress relaxation or creep can lead to the simultaneous measurement of fibril strain with macroscopic stress and strain. Sasaki and colleagues showed [40] that the majority of the changes in the X-ray diffraction spectrum could be explained by elongation of tropocollagen molecules, rather than intrafibrillar slippage of adjacent molecules or by increase of the gap (separation) region between axially separated fibrils. However, both earlier [45] and later [39] studies using similar methods have indicated that alterations in the gap/overlap ratio (indicative of intrafibrillar sliding) is playing a role in tendon deformation, as seen from changes in the relative intensities of different Bragg peaks in the SAXD spectrum. High strain rate deformation of tendon [52] found that intrafibrillar sliding and damage preceded macroscopic failure, as well as identifying a maximum D-period (for tendon collagen) of 68.4 nm below which all changes in fibrillar D-period were reversible.

The viscoelastic nature of the extrafibrillar matrix was demonstrated by [53], who showed that deformation in tendon could be modelled via assumptions of largely elastic fibrils and largely viscous interfibrillar matrices. When the collagen cross-linking was reduced, the situation reversed, with collagen fibrils now being much more viscous than the matrix. A combination of synchrotron and confocal testing of tendon during stress relaxation [42] was able to quantify the degree of fibrillar and fibre relaxation at different levels of macroscopically applied relaxation strains (Fig. 1.10). A two-level viscoelastic model, exhibiting the multiscale decay observed in tendon, was used to explain the data (Fig. 1.11). Intriguingly, however, the *magnitude* of the fibrillar and fibre relaxation argue against the prior theory of significant interfibrillar sliding. It is observed that the amount of fibrillar and fibre relaxation are nearly the same, and are both much smaller the interfibre shear. Such a finding

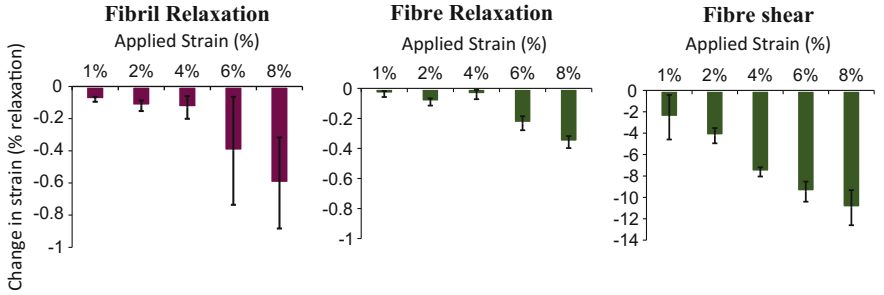

Fig. 1.10 Comparison of fibrillar and fibre strains and fibre shear during tensile deformation of tendon, measured via SAXD and confocal microscopy. Data from experiments reported in [42]

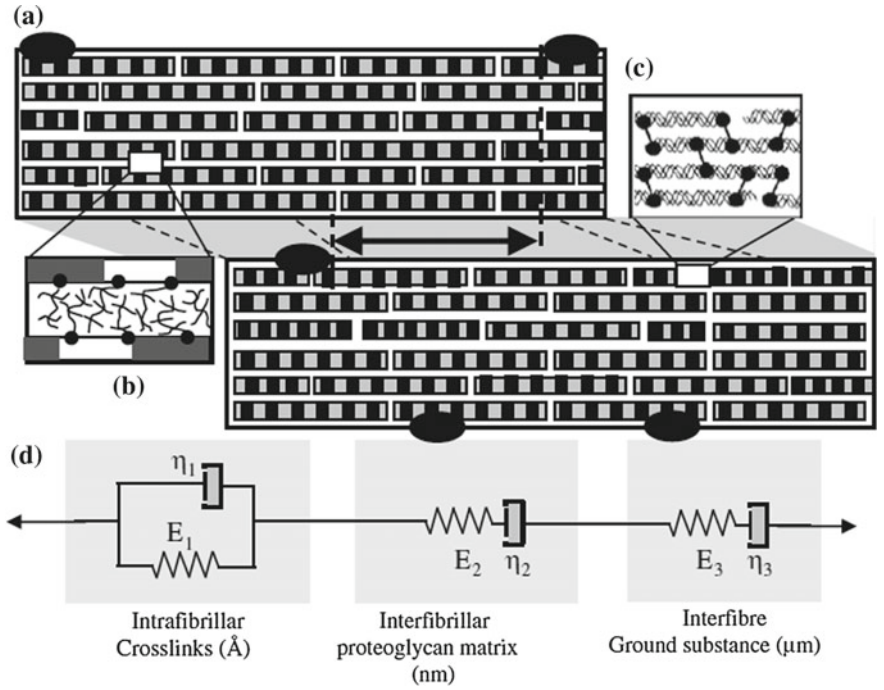

Fig. 1.11 A model of interfibrillar sliding during stress relaxation in tendons, based on *in situ* X-ray diffraction and confocal microscopy. Image taken with permission from [42]

would suggest that the fibrils within a fibre are deforming largely as one group, with little sliding between fibrils, and that a major contributor to sliding is the non-fibrous matrix at larger structural levels. Such results have stimulated renewed investigation into the viscoelastic properties of the IFM [54].

1.2.5 *Effects of Matrix Composition and Tendon Type*

Whilst general data describing tendon composition and mechanics have been covered thus far, recent data highlights the effect of matrix composition and tendon type. Tendon structure–function relationships can be investigated utilizing enzymatic digestion or knockout models, to establish how altered matrix composition influences tendon mechanics. Structurally, treatment of tendons in phosphate buffered saline (PBS) led to 20 % increase in water content and 11 % loss of GAG, while chondroitinase treatment led to 16 % increase in water content and 99 % loss of GAGs [56]. Interestingly, the swelling of samples or removal of GAGs had little discernible effect on gross tendon mechanics. However, the PBS swollen tendon samples showed significantly increased levels of fibril sliding, an effect which was negated by the removal of the GAG chains [55] (Fig. 1.12). More recently, biglycan and decorin knockout models of mice have also been adopted to investigate the role of GAGs in tendon mechanics. These have shown altered mechanical properties near the insertion site [57]. Whilst tendon quasi-static mechanics are little affected by changes to protoeglycans, viscoelastic properties show a number of changes. Fatigue resistance is lowered after GAG digestion, with more rapid stress relaxation as seen in Fig. 1.13a [58]. Whilst no significant viscoelastic phase shift was observed in patellar tendons from decorin knockout mice, it was noted that there was a tendency to increased stress relaxation levels with a reduction in the decorin level, as seen in Fig. 1.13b [59]. Studies into the effects of elastin have focused primarily on ligament, showing that removal of the small elastin component in ligament increases the length of the initial toe region of the stress–strain curve, suggesting that elastin primarily contributes to ligament function within the low load region, whilst failure properties are governed by collagen fibre failure [60]. Prior work on tendons and palmar aponeuroses showed a considerable reduction in modulus and increased hysteresis in elastase treated samples, whilst chondrotinase treatment appeared to reduce sample hysteresis [61].

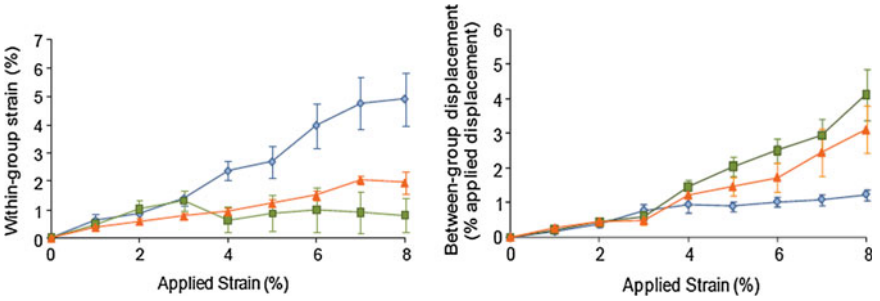

Fig. 1.12 Increased inter- and intrafibre sliding on removal of proteoglycans (digestion with chondroitinase ABC) in tendons. Data from [55]

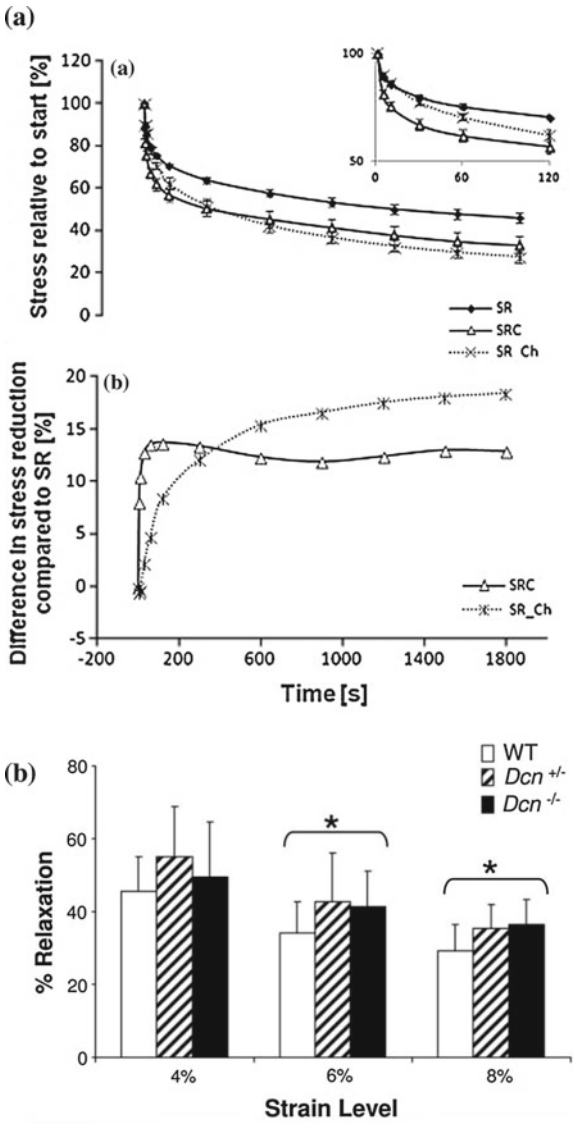

Fig. 1.13 **a** Greater stress relaxation in chondroitinase-digested tendon (main graph) versus controls (*inset*). Image reproduced with permission from [58]. **b** Increased percentage relaxation of tendon with both strain level and decorin removal (Dcn −/− is decorin knockout). Image reproduced with permission from [59]

In recent years, structure-function studies in tendon have focused on the clear functional differences between different tendons, looking to establish how structural variations are adopted to meet functional need. All tendons function to transfer muscle force to the skeleton and position limbs (positional tendons) but some have an additional role in locomotion, stretching to store energy which they can release back into the system to improve the efficiency of movement (energy storing tendons). Energy storing tendons, such as the Achilles tendon, or equine equivalent (the

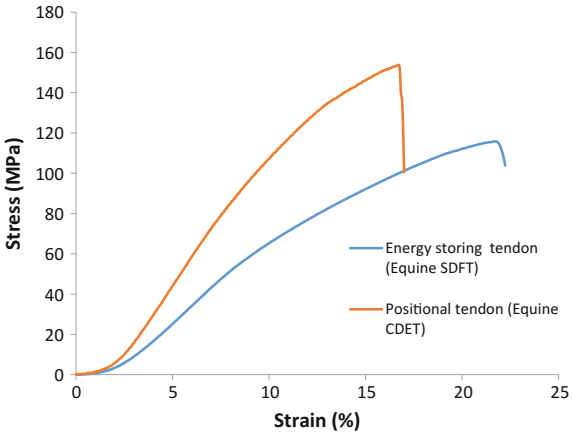

Fig. 1.14 Differences between stress–strain curves for energy storing and positional tendons; lower tangent modulus and maximum failure strain are observed in energy storing tendons

superficial digital flexor tendon—SDFT) [62, 63] are subjected to high strains and elastic recoil in use, and show high incidences of tendinopathy, whilst the low strains experienced by positional tendons make them less injury prone.

Energy storing tendons are less stiff and more extensible than positional tendons, facilitating energy storage and protecting the tendon from damage when subjected to large forces (Fig. 1.14) [64]. Furthermore, studies have additionally highlighted how energy storing tendons are significantly more fatigue resistant than positional tendons, enabling them to resist a greater degree of cyclic loading without damage (Fig. 1.15) [32]. Adopting hierarchical analysis techniques, it is possible to investigate the structural adaptations of energy storing tendons that facilitate these altered mechanics.

Data have highlighted that fibril and fibre sliding is less apparent in energy storing tendons, and that extension in these tendons adopts fascicle level sliding, mediated by the IFM [64]. The IFM is rich in elastin and lubricin to facilitate sliding and recoil behaviour (Fig. 1.16) [65], and levels of both of these proteins are higher in the IFM of energy storing tendons, resulting in significantly more fatigue resistant IFM in these samples [32, 54] (Fig. 1.17).

Fascicles within energy storing tendons are also helically arranged, providing additional resistance to fascicle damage as energy storing tendons are subjected to greater cyclical loads [66]. Interestingly, studies in ageing energy storing tendons have highlighted how these functional specialisms are lost with ageing. The helical organization of fascicles is reduced, whilst the IFM becomes stiffer, perhaps providing insight into the increased injury-risk seen in aged energy storing tendons [67].

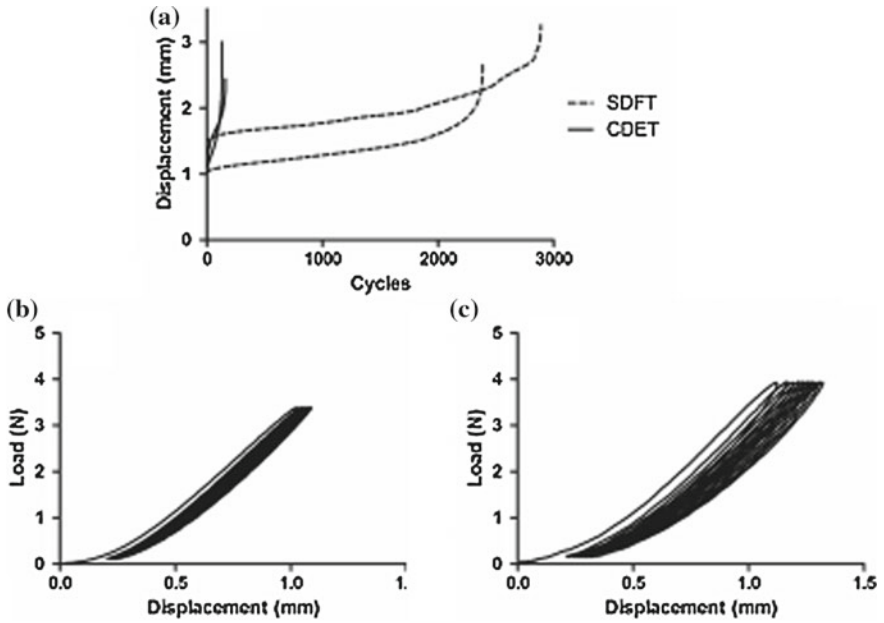

Fig. 1.15 **a** Creep curves for fascicles from superficial digital flexor and common digital extensor tendons (respectively SDFT and CDET) **b** and **c** Loading and unloading curves for the first 10 cycles for SDFT and CDET respectively. Data from [32]

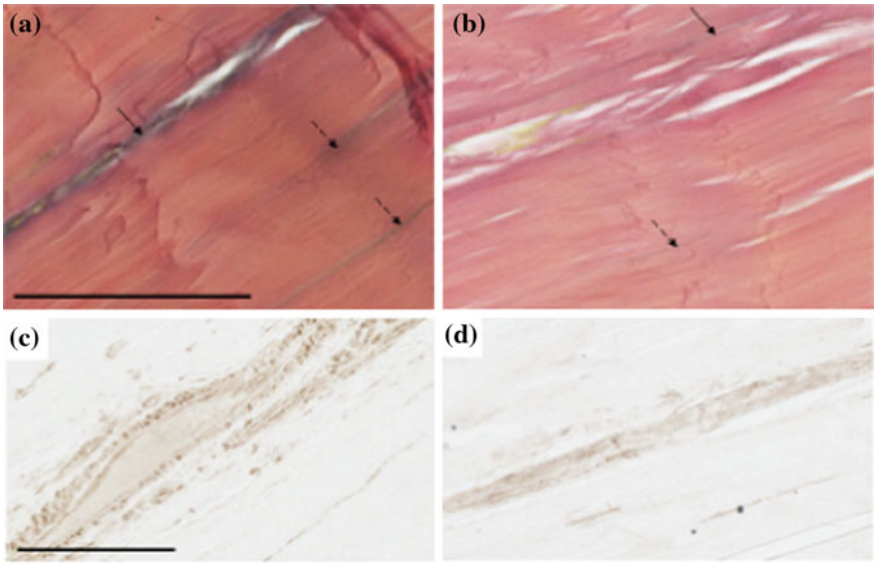

Fig. 1.16 Elastic von Giesons stained SDFT and CDET tissue (**a** and **b** respectively), with elastic fibres viewed as *blue/black lines*. SDFT exhibits elastin staining in the IFM (*solid arrow*) and a little inside the fascicles (dashed arrows). Lower numbers of elastic fibres are evident in CDET. **c** and **d** Immunohistochemical staining of lubricin in the IFM and within the fascicles of SDFT and CDET, showing considerable lubricin staining in the IFM of SDFT

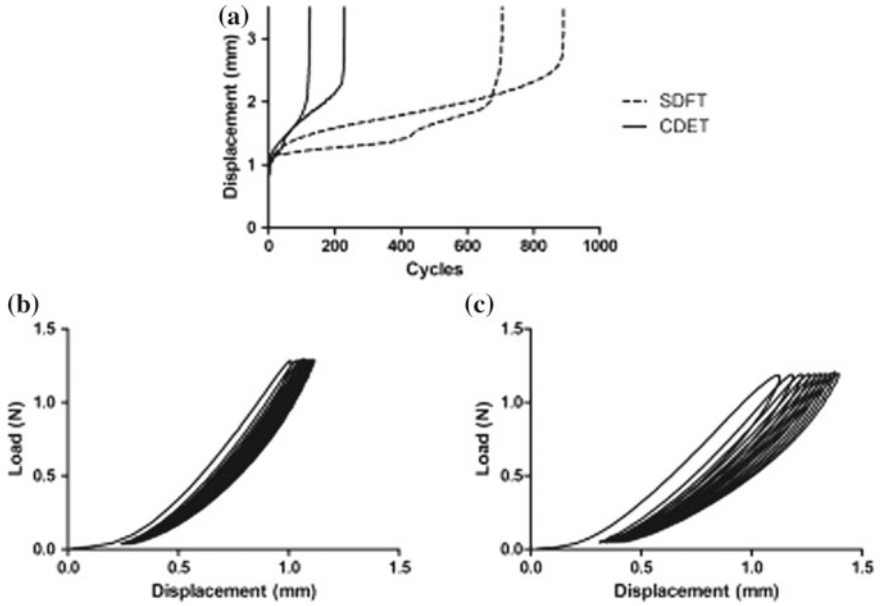

Fig. 1.17 **a** Creep curves for the interfascicular matrix (IFM) from SDFT and CDET tendons **b** and **c** Loading and unloading curves for the first 10 cycles for SDFT and CDET respectively [32, 54]

1.3 Heart Valves and Their Mechanical Properties

1.3.1 Types of Heart Valves

Heart valves enable the unidirectional flow of blood through the heart. There are four valves: the mitral, aortic, pulmonary and tricuspid. The tricuspid valve is between right atrium and right artery, the pulmonary valve between the right ventricle and pulmonary artery, the aortic valve between the left ventricle and the aorta and the mital valve between left atrium and left ventricle. Heart valves are passive structures, which open and close in response to the surrounding haemodynamic environment. The valve mechanics are reflective of the differences in pressures on the left and right hand side of the heart, with an overall × eightfold higher baseline pressure on the left side of the heart leading to more fatigue resistance in the aortic and mitral valves.

An alternate series of valves opening and closing occurs over a cardiac cycle. During the diastolic phase, the pressure in the ventricles is below atrial pressure. As a result, the mitral and tricuspid valves open, allowing blood flow from atria to ventricles. Concurrently, the aortic and pulmonary valves close to prevent a reverse flow of blood into either the aorta or pulmonary artery. In the systole, the atrium first contracts to push any remaining blood to ventricles. This is followed by ven-

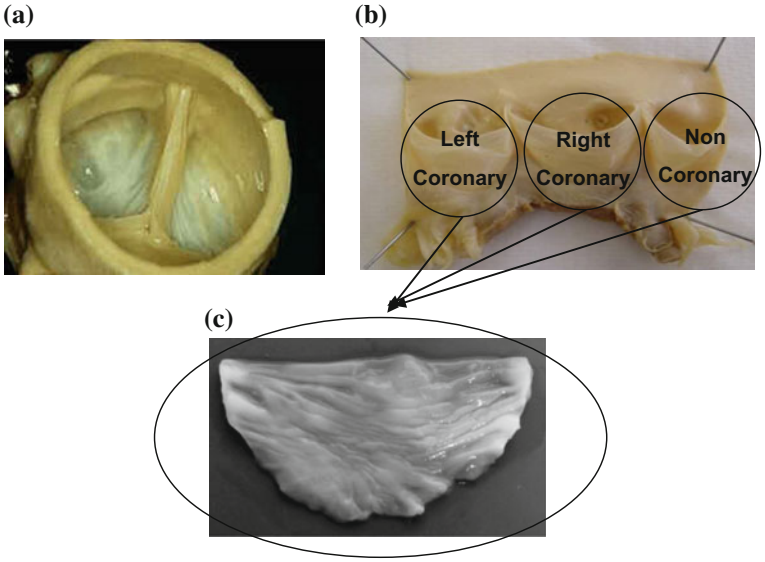

Fig. 1.18 **a** Photograph of an aortic valve **b** an unfolded valve opened to show the three coronary leaflets. **c** An unfolded leaflet showing the curved shape and anisotropic structure

tricular contraction, pushing blood into circulation, at which point the mitral and tricuspid valves close to prevent blood flowing back into the atria while the aortic and pulmonary valves open.

The aortic valve, also known as the semilunar valve, is shown in Fig. 1.18. In the aortic and pulmonary valve, three semicircular coronary leaflets are present, which flex against the walls of the aorta as blood flows out of the heart, but coapt perfectly as the valve closes to prevent backflow. By contrast, the mitral and tricuspid valves are called the atrio-ventricular valves, owing to their location between the atria and ventricle of both sides of the heart. The mitral valve has two primary leaflets, known as anterior and posterior leaflets, whilst the tricuspid valve has three. In both valves, the leaflets are corrugated, with the corrugations called scallops. The attachment of the valve leaflets to the papillary ventricular muscles are via a special type of tendinous structures known as chordae tendinae. The chordae tendinae are required to prevent the valve leaflets from inverting under applied pressure (prolapse). The mitral and aortic valves, being located on the high pressure side of the heart, are more prone to damage and hence have been subjected to more attention from a bioengineering standpoint. In contrast the tricuspid and pulmonary valves are on the low pressure side of the heart and have a lower incidence of damage.

1.3.2 Heart Valve Disorders

There are two main diseases or disorders which affect heart valve function: stenosis and regurgitation. Stenosis is the narrowing of the valve opening, limiting the flow of blood, and is usually a result of valve stiffening. The etiology may involve rheumatic fever or congenital defects. Regurgitation is when the valve does not close properly, and can be caused by failure of chordae tendinae, enlargement of surrounding heart structures, infections or Ehlers–Danlos syndrome. In general, these disorders affect the highly loaded aortic and mitral valves, with the mitral valve commonly regurgitating and the aortic valve often undergoing stenosis.

A stenotic aortic valve cannot flex out of the way as easily when blood is pushed out of the heart, meaning the left ventricle must generate higher pressure with each contraction, leading to muscular thickening of left ventricle walls and eventual dilation of the left ventricle and deterioration of systolic function. Congenital bicuspid aortic valve formation occurs during pregnancy when two aortic leaflets fuse together. It affects about 1–2 % of the general population and the altered valve mechanics increases valve calcification rates. Mitral valve regurgitation is the most common valve disorder. It usually occurs as a result of the chordae tendinae stretching over time to the point at which they can no longer hold the mitral valve leaflets in place, but allow them to invert or prolapse during systole.

1.3.3 Structure Function Relations in Aortic Valves

In aortic valves there is a consistent high pressure environment on both sides of the valve. The valve undergoes high, multidirectional strains and must rapidly open and close, necessitating flexion. Structurally, the valve is a corrugated trilayer structure, as shown schematically in (Fig. 1.19). At the top, a collagen rich layer (*fibrosa*)

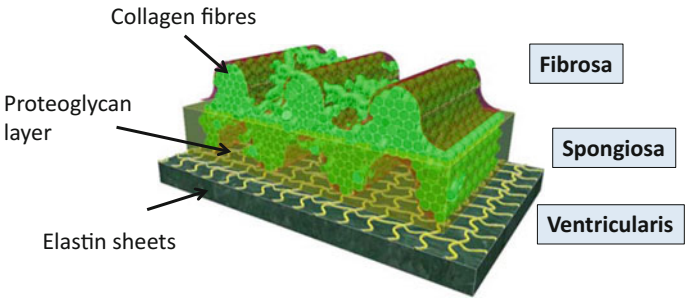

Fig. 1.19 Schematic model of the layered structure of the aortic valve leaflet. The collagen fibrils are shown as *green* rods, in a ridged/corrugated structure. The elastin fibres form a cross-linked network at the base of the valve layer in the ventricularis

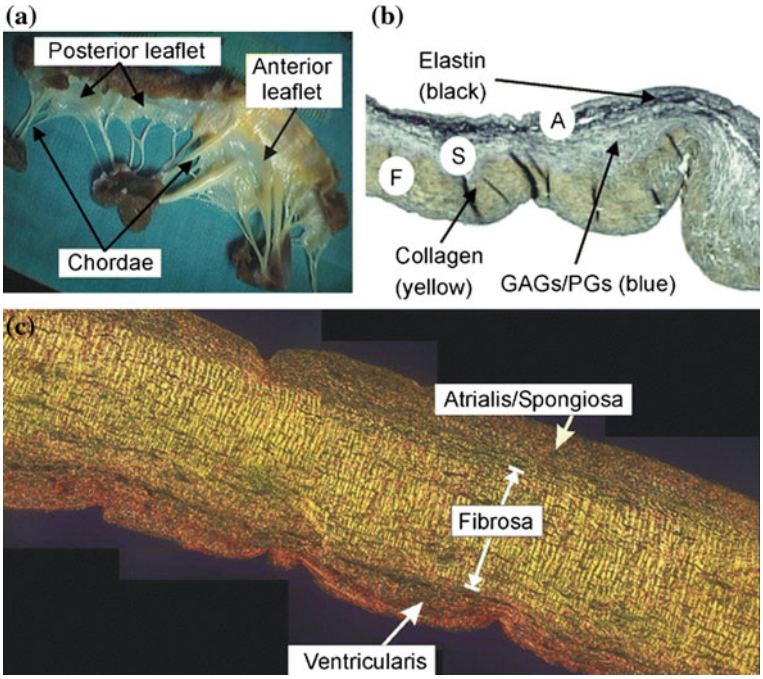

Fig. 1.20 **a** An image of a sectioned mitral valve, where the chordae tendinae and leaflets are clearly visible **b** Pentachrome stained cross-sections of mitral valves showing the different tissue layers. The elastic fibres are shown in *black*, the collagen in *yellow* and the PG/GAG phase in *blue* **c** Polarized light microscopy showing the different fibre texture and density in the ventricularis, fibrosa and spongiosa. (Image reproduced with permission from [68]

contains a multidirectional set of collagen fibres providing tensile strength. In the middle layer (*spongiosa*) a high proportion of proteoglycans allow other layers to shear, enabling large flexion. In the bottom layer (*ventricularis*), the elastin-rich layer provides considerable extension and recoil. The collagen fibres in the fibrosa form coarse bundles which run across the width of the valve, providing the corrugations that are characteristic of valve leaflets. Typically, the fibrosa is the thickest layer, as shown in Fig. 1.20. Confocal microscopy of the different layers of the aortic valve shows clearly the orientation differences as well as the degree of crimping (Fig. 1.21).

1.3.4 Structure Function Relations in Mitral Valves

The mitral valve structure is clinically important as it is more often repaired than replaced, hence the need to design a correct annulus. During the cardiac cycle, there is a significant pressure difference between the atrial and ventricular side of the valve, and the mitral valve must open and close with little resistance, but not pro-

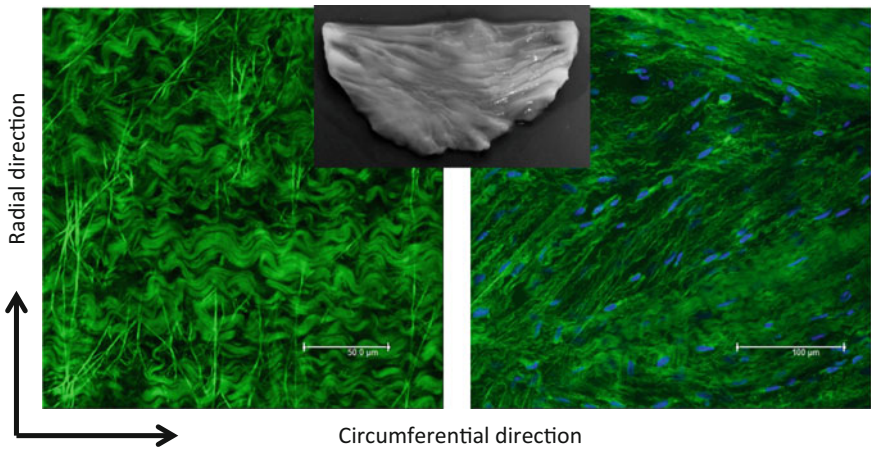

Fig. 1.21 Confocal microscopy of aortic valve leaflet layers showing the corrugated fibrosa region on the *left* and the underlying elastin-rich ventricularis on the *right* (Screen et al. unpublished work)

lapse against high pressure in the ventricle. During the heart beat, the annulus of the mitral valve can change shape significantly, going from circular at ventricular diastole to kidney shaped at peak systole. Structurally, the mitral valve is (in cross-section) a four-layered structure, with looser, elastin-rich layers at either external surface (ventricularis and atrialis) while the interior of the valve contains the collagen rich fibrosa and proteoglycan-rich spongiosa. Smooth muscle cells, nerve fibres and vascular channels are also present.

As seen in histological and microscopic images [69], mitral valves with deteriorated structure exhibit leaflet thickening and elongation of tendinous chords. In cross-section, it is seen that floppy mitral valves show very few collagen fibres in the central fibrosa region, significantly reducing the tensile resistance of the valve and making it more prone to collapse.

1.3.5 Anisotropic Structure and Mechanical Implications

The shape and structure of heart valves, with multiple leaflets, each composed of microscopically distinct layers, means that in order to understand the structure–function relations in this complex tissue, a range of mechanical test methods must be utilized. These can include uniaxial, biaxial and multiaxial tensile testing, with either point loading or pressurized loading in addition to testing with flexion. These will be briefly described in the following text:

Uniaxial mechanical properties In carrying out a uniaxial tensile test on a valve, one must first define a principal axis of loading. Despite the complex curved shape of each valve leaflet, two main directions can be defined, with respect to the position of the valve in its native state (Fig. 1.22a). The first, along the direction perpendicular to

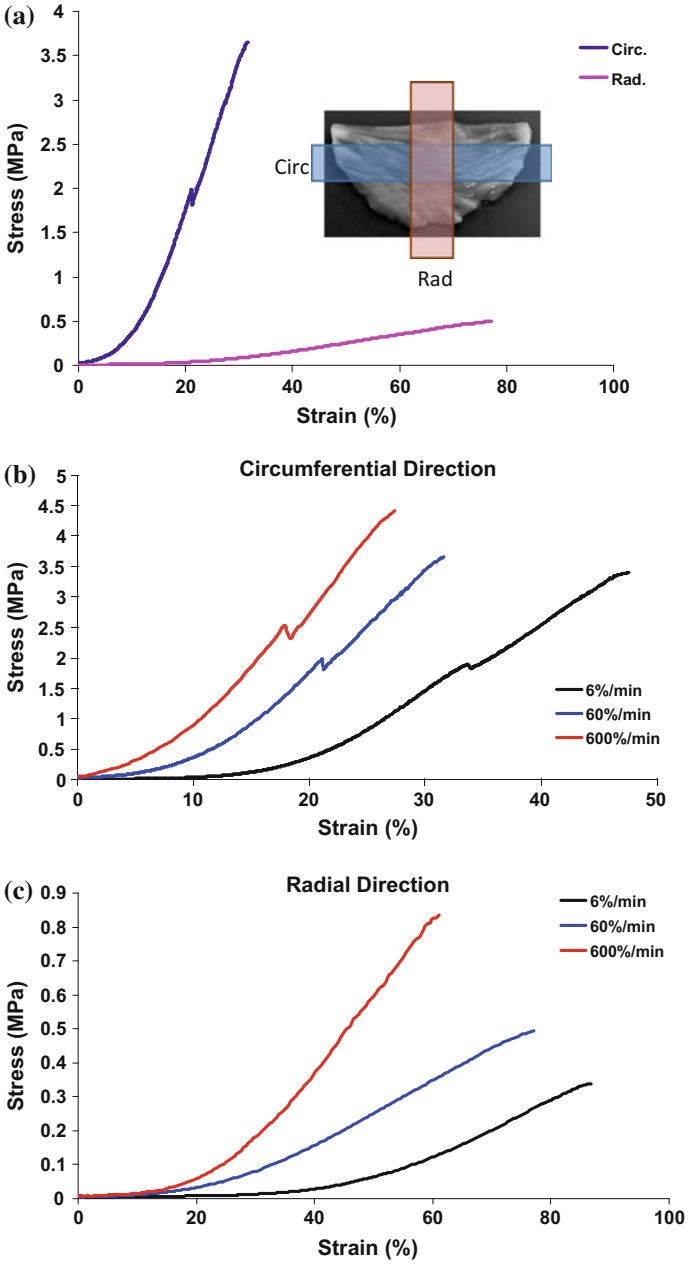

Fig. 1.22 **a** Uniaxial mechanical test of aortic heart valve leaflet tissue in the circumferential direction (*blue*) shows much higher stiffness, lower maximum strain and higher maximum stress compared to radial direction (*pink*). **b** and **c** Increasing strain rate significantly increases stiffness, reduces maximum strain and increases maximum stress. Inset: photograph of aortic valve, with sample sections along the circumferential and radial direction indicated

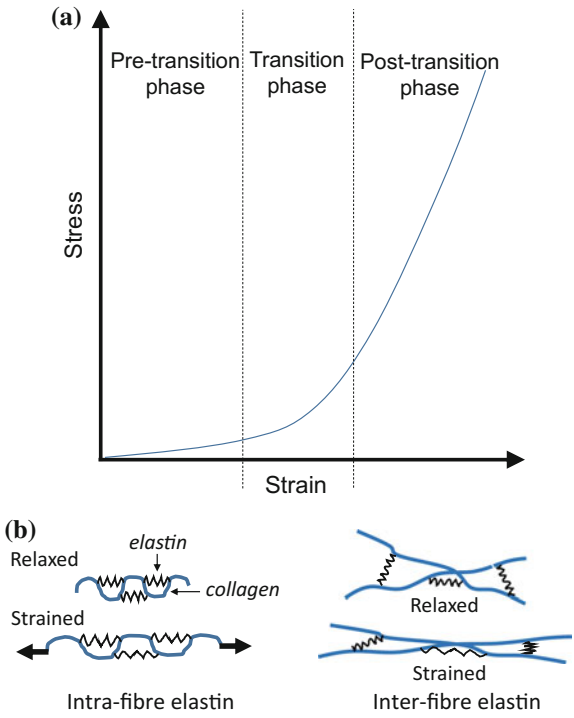

Fig. 1.23 **a** Schematic of tensile deformation of heart valves, showing three distinct zones of deformation with different tangent moduli. **b** The proposed collagen–elastin linkage model of [71]. Figure after [71]

the blood flow, is called the circumferential direction, while the second, which follows the main blood flow direction is called the radial direction. Tensile test curves from the longitudinal and radial directions are shown in Fig. 1.22a. It is observed that the maximum tangent modulus of the circumferential (C) sample is much larger than the radial (R) sample. This difference is mainly because there is a greater proportion of the collagen fibres along the loading direction in the C- than in the R-direction.

Both directions show strong strain rate sensitivity, with an increasing tangent modulus with strain rate observed in each case (Fig. 1.22b, c). Tests are normally carried out on strips running through the centre of the leaflet, but it is possible to cut circumferential or radial strips across a leaflet, with data showing the middle strip is stiffest in both cases [70].

To relate these mechanical data to the prior discussion on tendons, it is useful to divide the stress–strain curve schematically into three regions as shown in Fig. 1.23a. In the pre-transition phase, there is straightening of macro-crimp with elastin providing the main resistance to extension. In the middle (transition or heel region) the collagen fibres are progressively recruited to bear load and oriented in the loading direction. In the post-transition region (which is also closer to a linear stress–strain curve than the previous two) there is elastic extension.

Scott and Vesely [71] have proposed a linkage between the elastin and collagen fibres to enable recoil or return of the connective tissues in the heart valve. As per

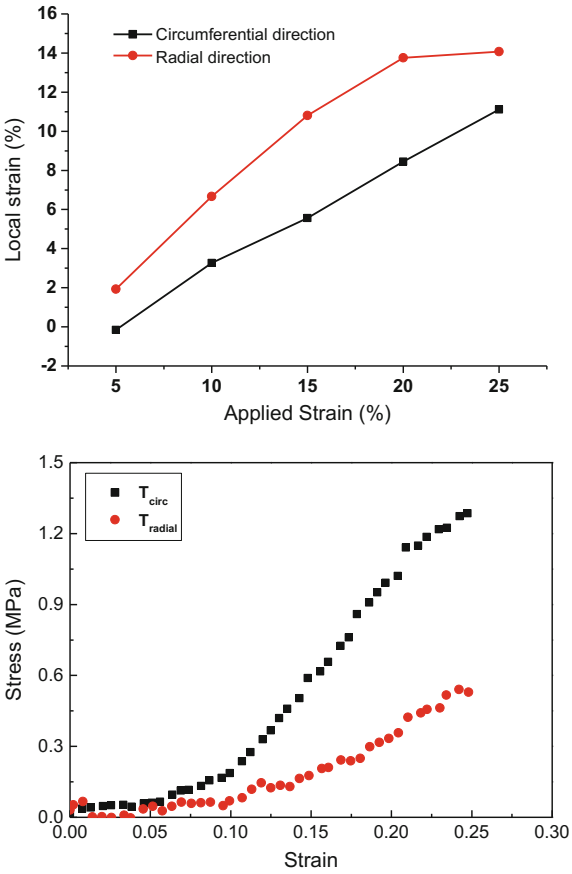

Fig. 1.24 Anisotropy of stress–strain response to biaxial deformation of aortic heart valves leaflet (Screen et al. unpublished work)

the mechanisms sketched in Fig. 1.23b, the interfibre connections via rubbery elastin linkages may enable the collagen bundles to return to their crimped state when relaxed.

Biaxial mechanical properties Biaxial mechanical testing protocols of heart valves, incorporating in-plane shear, have been described in [72]. Gripping is achieved via sutures so as not to constrain deformation in either direction. To ensure noncontact measurement of strain, marks are placed in a grid on the sample surface, and the attachment to the valve is via hooks which insert into the side of the tissue. Using a similar protocol, Screen et al. (unpublished) show that the local strain is larger in the radial direction compared to the circumferential direction (Fig. 1.24). Such a result is expected based on the predominant fibre orientation in the circumferential direction increasing the stress and stiffness along this axis. Likewise, an increased stress is observed in the circumferential direction.

Flexural mechanical properties Flexural mechanical tests on heart valves can measure the flexural stiffness either by bending with the curvature direction or against

it. Bending against curvature leads to larger stresses (0.70 ± 0.13 MPa) than bending with curvature (0.50 ± 0.13 MPa) [73]. Bending with curvature is dominated by tension in the ventricularis layer with little support from the fibrosa. This is because the fibrous layer is on the concave inner surface of the valve, as a result of which it is placed under compression when bending with curvature. Conversely, when the valve is bent against curvature the fibrosa is placed under tensile loading, which it can resist more effectively. Owing to the predominance of collagen in the fibrosa the modulus is higher in this case.

Enzymatic digestion tests Analogous to the enzymatic digestion testing described earlier for tendon, the removal of different ECM components of heart valves have a significant effect on the mechanics [74]. Elastin digestion of heart valves results in lowered modulus, increased extensibility in both circumferential and radial directions, and in each separate layer: fibrosa, spongiosa and ventricularis.

1.4 Conclusion

The hierarchical nature of connective tissues, together with the widely differing mechanical properties of the constituent elements, make the assignment of material parameters a challenging and scale-dependent problem. Methodologies to address these will be discussed in companion chapters of this volume. Here we note that on the experimental side, the use of multiscale analysis techniques (including microscopy and spectroscopy) may provide quantitative information on the stiffness and strain at different length scales, to be used together with modelling methodologies.

References

1. Vincent, J. F. V. (2012). *Structural biomaterials*. Princeton University Press.
2. Meyers, M. A., Chen, P.-Y., Lin, A. Y.-M., & Seki, Y. (2008). Biological materials: Structure and mechanical properties. *Progress in Materials Science*, *53*, 1–206.
3. Wainwright, S. A. (1982). *Mechanical design in organisms*. Princeton University Press.
4. Vrhovski, B., & Weiss, A. S. (1998). Biochemistry of tropoelastin. *European Journal of Biochemistry*, *258*(1), 1–18.
5. Yigit, S., Dinjaski, N., & Kaplan, D. L. (2015). Fibrous proteins: At the crossroads of genetic engineering and biotechnological applications. *Biotechnology and Bioengineering*.
6. Hulmes, D. J. S. (2008). Collagen diversity, synthesis and assembly. In P. Fratzl (Ed.), *Collagen: Structure and mechanics* (pp. 15–47). New York: Springer Science+Business Media.
7. Meek, K. M., Chapman, J. A., & Hardcastle, R. A. (1979). The staining pattern of collagen fibrils. Improved correlation with sequence data. *Journal of Biological Chemistry*, *254*(21), 10710–10714.
8. Kadler, K. E., Holmes, D. F., Graham, H., & Starborg, T. (2000). Tip-mediated fusion involving unipolar collagen fibrils accounts for rapid fibril elongation, the occurrence of fibrillar branched networks in skin and the paucity of collagen fibril ends in vertebrates. *Matrix Biology*, *19*(4), 359–365.

9. Screen, H. R. C., Lee, D. A., Bader, D. L., & Shelton, J. C. (2004). An investigation into the effects of the hierarchical structure of tendon fascicles on micromechanical properties. *Proceedings of the Institution of Mechanical Engineers, Part H: Journal of Engineering in Medicine*, *218*(2), 109–119.
10. Weiner, S., Traub, W., & Wagner, H. D. (1999). Lamellar bone: Structure-function relations. *Journal of Structural Biology*, *126*(3), 241–255.
11. Green, E. M., Mansfield, J. C., Bell, J. S., & Winlove, C. P. (2014). The structure and micromechanics of elastic tissue. *Interface Focus*, *4*(2), 20130058.
12. Daamen, W. F., Veerkamp, J. H., Van Hest, J. C. M., & Van Kuppevelt, T. H. (2007). Elastin as a biomaterial for tissue engineering. *Biomaterials*, *28*(30), 4378–4398.
13. Raabe, D., Sachs, C., & Romano, P. (2005). The crustacean exoskeleton as an example of a structurally and mechanically graded biological nanocomposite material. *Acta Materialia*, *53*(15), 4281–4292.
14. Fabritius, H.-O., Sachs, C., Triguero, P. R., & Raabe, D. (2009). Influence of structural principles on the mechanics of a biological fiber-based composite material with hierarchical organization: The exoskeleton of the lobster homarus americanus. *Advanced Materials*, *21*(4), 391–400.
15. Sanchez, C., Arribart, H., & Guille, M. M. G. (2005). Biomimetism and bioinspiration as tools for the design of innovative materials and systems. *Nature Materials*, *4*(4), 277–288.
16. Hull, D., Clyne, T. W. (1996). An introduction to composite materials. Cambridge university press.
17. Cox, H. L. (1952). The elasticity and strength of paper and other fibrous materials. *British Journal of Applied Physics*, *3*(3), 72.
18. Chuong, C. J., & Fung, Y. C. (1986). Residual stress in arteries. In *Frontiers in biomechanics* (pp. 117–129). Springer.
19. Korhonen, R. K., Laasanen, M. S., Töyräs, J., Lappalainen, R., Helminen, H. J., & Jurvelin, J. S. (2003). Fibril reinforced poroelastic model predicts specifically mechanical behavior of normal, proteoglycan depleted and collagen degraded articular cartilage. *Journal of Biomechanics*, *36*(9), 1373–1379.
20. Blevins, F. T. (1996). Structure, function, and adaptation of tendon. *Current Opinion in Orthopaedics*, *7*(6), 57–61.
21. Riley, G. P., Harrall, R. L., Cawston, T. E., Hazleman, B. L., & Mackie, E. J. (1996). Tenascin-C and human tendon degeneration. *The American Journal of Pathology*, *149*(3), 933.
22. Benjamin, M., & Ralphs, J. R. (1997). Tendons and ligaments—an overview. *Histology and Histopathology*, *12*(4), 1135–1144.
23. Smith, R. K. W., Zunino, L., Webbon, P. M., & Heinegård, D. (1997). The distribution of cartilage oligomeric matrix protein (COMP) in tendon and its variation with tendon site, age and load. *Matrix Biology*, *16*(5), 255–271.
24. Yoon, H. J., & Halper, J. (2005). Tendon proteoglycans: Biochemistry and function. *J Musculoskelet Neuronal Interact*, *5*(1), 22–34.
25. Thorpe, C. T., Birch, H. L., Clegg, P. D., & Screen, H. R. C. (2013). The role of the non-collagenous matrix in tendon function. *International Journal of Experimental Pathology*, *94*(4), 248–259.
26. Kastelic, J., Galeski, A., & Baer, E. (1978). The multicomposite structure of tendon. *Connective Tissue Research*, *6*(1), 11–23.
27. Dyer, R. F., & Enna, C. D. (1976). Ultrastructural features of adult human tendon. *Cell and Tissue Research*, *168*(2), 247–259.
28. Ramachandran, G. N. (1988). Stereochemistry of collagen. *International Journal of Peptide and Protein Research*, *31*(1), 1–16.
29. Orgel, J. P. R. O., Irving, T. C., Miller, A., & Wess, T. J. (2006). Microfibrillar structure of type I collagen in situ. *Proceedings of the National Academy of Sciences*, *103*(24), 9001–9005.
30. Goh, K. L., Holmes, D. F., Lu, H.-Y., Richardson, S., Kadler, K. E., Purslow, P. P., et al. (2008). Ageing changes in the tensile properties of tendons: Influence of collagen fibril volume fraction. *Journal of Biomechanical Engineering*, *130*(2), 021011.

31. Scott, J. E. (2003). Elasticity in extracellular matrix "shape modules" of tendon, cartilage, etc. A sliding proteoglycan-filament model. *The Journal of Physiology*, *553*(2), 335–343.
32. Thorpe, C. T., Riley, G. P., Birch, H. L., Clegg, P. D., & Screen, H. R. C. (2016). Fascicles and the interfascicular matrix show adaptation for fatigue resistance in energy storing tendons. *Acta Biomaterialia*.
33. Buckwalter, J. A., Einhorn T. A., & Simon, S. R. (2000). *Orthopaedic basic science: Biology and biomechanics of the musculoskeletal system* (vol. 1). Amer Academy of Orthopaedic.
34. Kastelic, J., Palley, I., & Baer, E. (1980). A structural mechanical model for tendon crimping. *Journal of Biomechanics*, *13*(10), 887–893.
35. Smith, L., Xia, Y., Galatz, L. M., Genin, G. M., & Thomopoulos, S. (2012). Tissue-engineering strategies for the tendon/ligament-to-bone insertion. *Connective Tissue Research*, *53*(2), 95–105.
36. Gupta, H. S. (2008). Nanoscale deformation mechanisms in collagen. In P. Fratzl (Ed.), *Collagen: Structure and mechanics* (pp. 155–173). New York: Springer Science+Business Media.
37. Misof, K., Rapp, G., & Fratzl, P. (1997). A new molecular model for collagen elasticity based on synchrotron x-ray scattering evidence. *Biophysical Journal*, *72*(3), 1376.
38. Atkinson, T. S., Ewers, B. J., & Haut, R. C. (1999). The tensile and stress relaxation responses of human patellar tendon varies with specimen cross-sectional area. *Journal of Biomechanics*, *32*(9), 907–914.
39. Fratzl, P., Misof, K., Zizak, I., Rapp, G., Amenitsch, H., & Bernstorff, S. (1998). Fibrillar structure and mechanical properties of collagen. *Journal of Structural Biology*, *122*(1), 119–122.
40. Sasaki, N., & Odajima, S. (1996). Elongation mechanism of collagen fibrils and force-strain relations of tendon at each level of structural hierarchy. *Journal of Biomechanics*, *29*(9), 1131–1136.
41. Wang, X. T., & Ker, R. F. (1995). Creep rupture of wallaby tail tendons. *Journal of Experimental Biology*, *198*(3), 831–845.
42. Gupta, H. S., Seto, J., Krauss, S., Boesecke, P., & Screen, H. R. C. (2010). In situ multi-level analysis of viscoelastic deformation mechanisms in tendon collagen. *Journal of Structural Biology*, *169*(2), 183–191.
43. Sasaki, N., & Odajima, S. (1996). Stress-strain curve and Young's modulus of a collagen molecule as determined by the X-ray diffraction technique. *Journal of Biomechanics*, *29*(5), 655–658.
44. Masic, A., Bertinetti, L., Schuetz, R., Chang, S.-W., Metzger, T. H., Buehler, M. J., et al. (2015). Osmotic pressure induced tensile forces in tendon collagen. *Nature Communications*, *6*.
45. Mosler, E., Folkhard, W., Knörzer, E., Nemetschek-Gansler, H., Nemetschek, T., & Koch, M. H. J. (1985). Stress-induced molecular rearrangement in tendon collagen. *Journal of Molecular Biology*, *182*(4), 589–596.
46. Sasaki, N., Shukunami, N., Matsushima, N., & Izumi, Y. (1999). Time-resolved X-ray diffraction from tendon collagen during creep using synchrotron radiation. *Journal of Biomechanics*, *32*(3), 285–292.
47. Eppell, S. J., Smith, B. N., Kahn, H., & Ballarini, R. (2006). Nano measurements with microdevices: Mechanical properties of hydrated collagen fibrils. *Journal of the Royal Society Interface*, *3*(6), 117–121.
48. Buehler, M. J. (2006). Nature designs tough collagen: Explaining the nanostructure of collagen fibrils. *Proceedings of the National Academy of Sciences*, *103*(33), 12285–12290.
49. Scree, H. R. C., Lee, D. A., Bader, D. L., & Shelton, J. C. (2003). Development of a technique to determine strains in tendons using the cell nuclei. *Biorheology*, *40*, 361–368.
50. Screen, H. R. C., Bader, D. L., Lee, D. A., & Shelton, J. C. (2004). Local strain measurement within tendon. *Strain*, *40*(4), 157–163.
51. Szczesny, S. E., Caplan, J. L., Pedersen, P., & Elliott, D. M. (2015). Quantification of interfibrillar shear stress in aligned soft collagenous tissues via notch tension testing. *Scientific Reports*, *5*.

52. Knörzer, E., Folkhard, W., Geercken, W., Boschert, C., Koch, M. H. J., Hilbert, B., et al. (1986). New aspects of the etiology of tendon rupture. *Archives of Orthopaedic and Traumatic Surgery*, *105*(2), 113–120.
53. Puxkandl, R., Zizak, I., Paris, O., Keckes, J., Tesch, W., Bernstorff, S., et al. (2002). Viscoelastic properties of collagen: Synchrotron radiation investigations and structural model. *Philosophical Transactions of the Royal Society of London B: Biological Sciences*, *357*(1418), 191–197.
54. Thorpe, C. T., Godinho, M. S. C., Riley, G. P., Birch, H. L., Clegg, P. D., & Screen, H. R. C. (2015). The interfascicular matrix enables fascicle sliding and recovery in tendon, and behaves more elastically in energy storing tendons. *Journal of the Mechanical Behavior of Biomedical Materials*, *52*, 85–94.
55. Screen, H. R. C., Shelton, J. C., Chhaya, V. H., Kayser, M. V., Bader, D. L., & Lee, D. A. (2005). The influence of noncollagenous matrix components on the micromechanical environment of tendon fascicles. *Annals of Biomedical Engineering*, *33*(8), 1090–1099.
56. Screen, H. R. C., Chhaya, V. H., Greenwald, S. E., Bader, D. L., Lee, D. A., & Shelton, J. C. (2006). The influence of swelling and matrix degradation on the microstructural integrity of tendon. *Acta Biomaterialia*, *2*(5), 505–513.
57. Connizzo, B. K., Sarver, J. J., Lozzo, R. V., Birk, D. E., & Soslowsky, L. J. (2013). Effect of age and proteoglycan deficiency on collagen fiber re-alignment and mechanical properties in mouse supraspinatus tendon. *Journal of Biomechanical Engineering*, *135*(2), 021019.
58. Legerlotz, K., Riley, G. P., & Screen, H. R. C. (2013). GAG depletion increases the stress-relaxation response of tendon fascicles, but does not influence recovery. *Acta Biomaterialia*, *9*(6), 6860–6866.
59. Dourte, L. A. M., Pathmanathan, L., Jawad, A. F., Lozzo, R. V., Mienaltowski, M. J., Birk, D. E., et al. (2012). Influence of decorin on the mechanical, compositional, and structural properties of the mouse patellar tendon. *Journal of Biomechanical Engineering*, *134*(3), 031005.
60. Henninger, H. B., Underwood, C. J., Romney, S. J., Davis, G. L., & Weiss, J. A. (2013). Effect of elastin digestion on the quasi-static tensile response of medial collateral ligament. *Journal of Orthopaedic Research*, *31*(8), 1226–1233.
61. Millesi, H., Reihsner, R., Hamilton, G., Mallinger, R., & Menzel, E. J. (1995). Biomechanical properties of normal tendons, normal palmar aponeuroses, and tissues from patients with dupuytren's disease subjected to elastase and chondroitinase treatment. *Clinical Biomechanics*, *10*(1), 29–35.
62. Birch, H. L. (2007). Tendon matrix composition and turnover in relation to functional requirements. *International Journal of Experimental Pathology*, *88*(4), 241–248.
63. Ker, R. F., Wang, X. T., & Pike, A. V. (2000). Fatigue quality of mammalian tendons. *Journal of Experimental Biology*, *203*(8), 1317–1327.
64. Thorpe, C. T., Udeze, C. P., Birch, H. L., Clegg, P. D., & Screen, H. R. C. (2012) Specialization of tendon mechanical properties results from interfascicular differences. *Journal of the Royal Society Interface*, p. rsif20120362.
65. Thorpe, C. T., Karunaseelan, K. J., Ng Chieng Hin, J., Riley, G. P., Birch, H. L., Clegg, P. D., et al. (2016). Distribution of proteins within different compartments of tendon varies according to tendon type. *Journal of Anatomy*.
66. Thorpe, C. T., Klemt, C., Riley, G. P., Birch, H. L., Clegg, P. D., & Screen, H. R. C. (2013). Helical sub-structures in energy-storing tendons provide a possible mechanism for efficient energy storage and return. *Acta Biomaterialia*, *9*(8), 7948–7956.
67. Thorpe, C. T., Riley, G. P., Birch, H. L., Clegg, P. D., & Screen, H. R. C. (2014). Fascicles from energy-storing tendons show an age-specific response to cyclic fatigue loading. *Journal of the Royal Society Interface*, *11*(92), 20131058.
68. Grande-Allen, J. K., & Liao, J. (2011). The heterogeneous biomechanics and mechanobiology of the mitral valve: Implications for tissue engineering. *Current Cardiology Reports*, *13*(2), 113–120.
69. McCarthy, K. P., Ring, L., & Rana, B. S. (2010). Anatomy of the mitral valve: Understanding the mitral valve complex in mitral regurgitation. *European Heart Journal-Cardiovascular Imaging*, *11*(10), i3–i9.

70. Missirlis, Y. F., & Chong, M. (1978). Aortic valve mechanics-part I: Material properties of natural porcine aortic valves. *Journal of Bioengineering*, *2*(3–4), 287–300.
71. Scott, M., & Vesely, I. (1995). Aortic valve cusp microstructure: The role of elastin. *The Annals of Thoracic Surgery*, *60*, S391–S394.
72. Sacks, M. S. (1999). A method for planar biaxial mechanical testing that includes in-plane shear. *Journal of Biomechanical Engineering*, *121*(5), 551–555.
73. Merryman, D. W., Huang, H.-Y. S., Schoen, F. J., & Sacks, M. S. (2006). The effects of cellular contraction on aortic valve leaflet flexural stiffness. *Journal of Biomechanics*, *39*(1), 88–96.
74. Vesely, I. (1997). The role of elastin in aortic valve mechanics. *Journal of Biomechanics*, *31*(2), 115–123.